Drag reduction in open channel flow by aeration and suspended load

Réduction des pertes de frottement pour des écoulements à surface libre avec entraînement d'air et de sédiments

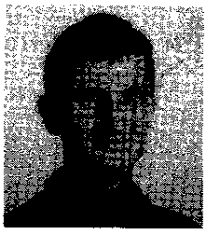

HUBERT CHANSON
Lecturer in Hydraulics/Fluid Mechanics,
Department of Civil Engineering,
The University of Queensland,
Brisbane QLD 4072, Australia

ABSTRACT
In supercritical open channel flows, air is entrained at the free surface. Such air-water flows, called self-aerated flows, exhibit smaller friction losses than non-aerated flows. New data on drag reduction in self-aerated flows are presented. It is shown that the drag reduction process is linked with the presence of an air concentration boundary layer next to the channel bottom. An analogy with dilute polymer solutions and micro bubble modified boundary layers is developed and it is suggested that the presence of air next to the bottom increases the effective viscosity of the mixture and the sublayer thickness.
A parallel with sediment laden flows is also developed. Although the distribution of suspended sediments differs from the distribution of air bubbles, it is suggested that the mechanisms of drag reduction observed in suspended sediment flows are similar to those in self-aerated flows.

RÉSUMÉ
Dans le cas d'écoulement à surface libre supercritique, une certaine quantité d'air est entraînée à la surface libre. De tels écoulements à surface libre avec entraînement d'air, sont caractérisés par des pertes de charge plus faibles. On présente de nouveaux résultats décrivant cette réduction du coefficient de perte de charge. L'auteur montre que le mécanisme de réduction des forces de frottement est lié à la présence d'une couche limite de bulles d'air près du fond du canal. On développe une analogie avec les écoulements de solutions diluées de polymers et avec les écoulement diphasiques dans une couche limite. La couche limite de bulles d'air induit une augmentation locale de la viscosité cinématique du fluide près de la paroi, et une expansion de la sous-couche laminaire (viscous sublayer).
L'auteur suggère que cette analogie peut être étendue aux écoulements avec suspension de matériaux, qui sont sujets, aussi, à des réductions du coefficient de frottement.

1 Introduction

For a spillway flow the upstream flow region is smooth and glassy. Next to the invert turbulence is generated and the boundary layer grows until the outer edge of the boundary layer reaches the surface (Fig. 1). From this location, called the point of inception, the turbulent velocity acting next to the free surface can initiate natural free surface aeration. This process is called self-aeration. The boundary layer becomes fully developed and extends up to the free surface. Downstream of the point of inception, a layer containing a mixture of both air and water extends gradually through the fluid. The rate of growth of the layer is small. From the point where the air

Revision received July 14, 1993. Open for discussion till August 31, 1994.

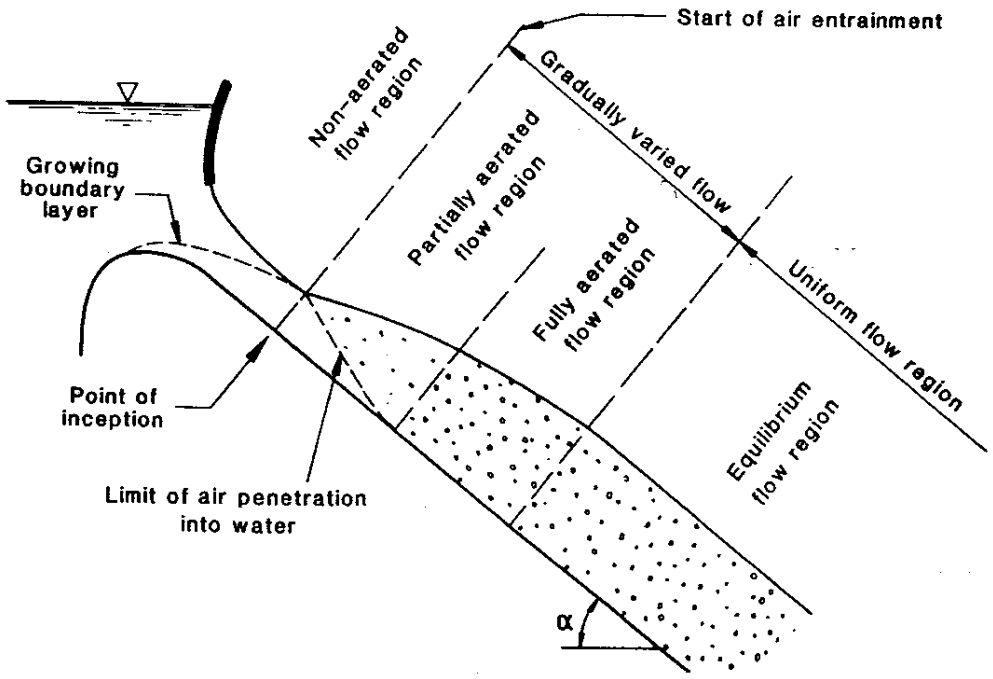

Fig. 1. Air entrainment along a spillway.
Entraînenement d'air aur long d'un coursier d'évacuateur de crues.

has reached the chute invert, the air concentration distribution continues to vary gradually with distance. Further downstream the air-water flow becomes uniform.

Self-aeration was studied initially because the entrained air increases the bulk of the flow (Falvey 1980). Further the presence of air reduces the friction losses (Wood 1983) and the resulting increase of flow momentum must be taken into account when designing a stilling basin downstream of a spillway. Also the presence of air in high velocity flows may be prevent or reduce the cavitation erosion damage to spillway surfaces (May 1987).

In the paper the characteristics of self-aerated flows are summarised in the first part. New results on drag reduction in self-aerated flows are discussed. Model and prototype data are presented. An analogy with dilute polymer solutions, micro-bubble modified boundary layers and sediment laden flows is developed.

Mechanisms of air entrainment

In high speed flows, air entrainment is caused by the turbulent velocity acting next to the air-water interface. Through this interface air is continuously being trapped and released, and the resulting air-water mixture may extend to the spillway invert. Air entrainment occurs when the turbulence level is large enough to overcome both surface tension and gravity effects: i.e., the turbulent velocity normal to the free surface v' must be large enough to overcome the surface tension pressure (Sene 1984, Ervine and Falvey 1987) and greater than the bubble rise velocity component for the bubble to be carried away. These conditions become:

$$v' > \sqrt{\frac{8\sigma}{\varrho_w d_b}} \tag{1}$$

and

$$v' > u_r \cos\alpha \tag{2}$$

where σ is the surface tension, ϱ_w is the water density, d_b is the air bubble diameter, u_r is the bubble rise velocity and α is the spillway slope. Air entrainment occurs when the turbulent velocity v' satisfies both equations (1) and (2). Assuming a rise velocity of 0.25 m/s, equations (1) and (2) suggest that self-aeration occurs for turbulent velocities normal to the free surface greater than 0.1 to 0.3 m/s, and bubbles in the range 8 to 40 mm are the most likely to be entrained. On prototype spillways the flow conditions are fully turbulent, and the conditions for free surface aeration are always satisfied when the growing boundary layer reaches the free surface. Downstream of the point of inception large quantities of air are entrained.

Definitions

The local air concentration C is defined as the volume of air per unit volume of air and water. The characteristic flow depth d is defined as:

$$d = \int_0^{Y_{90}} (1 - C)\, dy \tag{3}$$

where y is measured perpendicular to the spillway surface and Y_{90} is the depth where the local air concentration is 90%. The depth averaged mean air concentration C_{mean} is defined as:

$$(1 - C_{mean})\, Y_{90} = d \tag{4}$$

The average water velocity U_w is defined as:

$$U_w = \frac{q_w}{d} \tag{5}$$

where q_w is the water discharge per unit width. The characteristic velocity V_{90} is defined as that at Y_{90}.

2 Self-aerated flow characteristics

Downstream of the point of inception of air entrainment, the air concentration distribution can be represented by a diffusion model of the air bubbles within the air-water mixture (Wood 1984):

$$C = \frac{B'}{B' + \exp\left(-G' \cos \alpha y'^2\right)} \tag{6}$$

where B' and G' are functions of the mean air concentration only and $y' = y/Y_{90}$. Values of B' and G' were computed for Straub and Anderson's (1958) data. The results are presented in Table 1, columns 2 and 3 as functions of the mean air concentration (column 1).

Next to the spillway bottom, the data of Cain (1978) and Chanson (1988) depart from equation (6) and indicate that the air concentration tends to zero at the bottom (Fig. 2). The existence of an air concentration boundary layer is consistent with the data of Bodgevich et al. (1977), Madavan et al. (1984) and Marie et al. (1991) who studied the injection of micro-air-bubbles in turbulent boundary layer flows (Table 2). Their measurements of air bubble concentration distributions showed also that the bubble concentration falls off to zero at a solid boundary. A re-analysis of the data obtained by Bogdevich et al. (1977) and Cain (1978) shows that the air concentration distribution can be estimated in the air concentration boundary layer as:

$$C = C_b \left(\frac{y}{\delta_{ab}}\right)^{0.270} \tag{7}$$

Table 1. Air concentration and velocity distribution parameters in self-aerated flows
Coefficients des distributions de concentrations en air et de vitesses pour des écoulement à surface libre avec entraînement d'air

C_{mean} (1)	$G' * \cos\alpha$ (a) (2)	B' (a) (3)	C_b (b) (4)	$\frac{V_{90}\ Y_{90}}{q_w}$ (5)	f_e/f eq. (11) (6)
0.0	+ infinite	0.00	0.00	1.167	1.0
0.161	7.999	0.003021	0.02	1.453	0.964
0.241	5.744	0.028798	0.04	1.641	0.867
0.310	4.834	0.07157	0.07	1.805	0.768
0.410	3.825	0.19635	0.17	2.141	0.632
0.569	2.675	0.62026	0.36	2.985	0.430
0.622	2.401	0.8157	0.46	3.319	0.360
0.680	1.8942	1.3539	0.55	4.151	0.277
0.721	1.5744	1.8641	0.64	4.859	0.215

Notes: (a) computed from Straub and Anderson's (1958) data
(b) computed from equation (6): $C_b = B'/(B'+1)$

where δ_{ab} is the air concentration boundary layer thickness, and C_b is the air concentration at the outer edge of the air concentration boundary layer. C_b satisfies the continuity between equations (6) and (7): if $\delta_{ab} \ll Y_{90}$, C_b becomes: $C_b = B'/(B'+1)$ (table 1, column 4). Equation (7) is plotted on Fig. 3 and compared with experimental data.

For the data of Bogdevich et al. (1977), Cain (1978) and Chanson (1988), the air concentration boundary layer dimensionless thickness Δ_{ab} is plotted versus the Reynolds number $Re+$ on Fig. 4, where $\Delta_{ab} = \delta_{ab} V_*/\nu_w$, V_* is the shear velocity, ν_w is the kinematic viscosity of water, $Re+ = V_o Y_o/\nu_w$, V_o is the velocity outside the boundary layer, Y_o is the boundary layer thickness. For self-aerated flows, V_o and Y_o were taken as V_{90} and Y_{90}. The data shown on Fig. 4 were

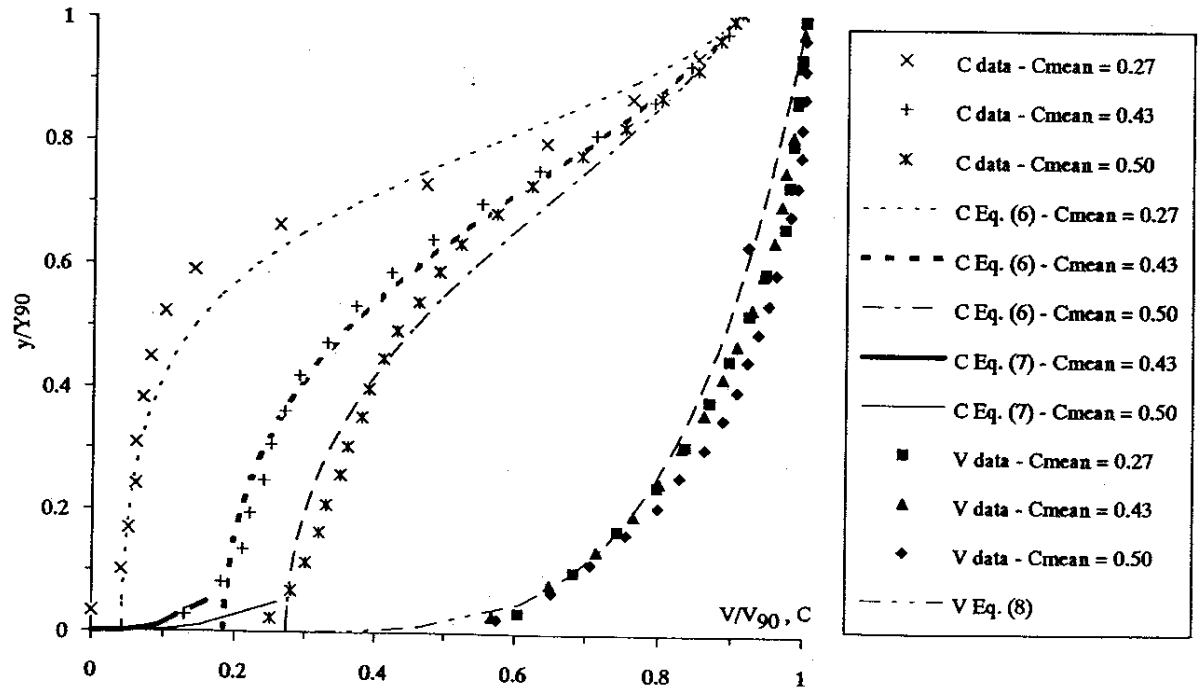

Fig. 2. Air concentration and velocity distributions at Aviemore spillway - Cain (1978).
Distributions de concentrations en air et de vitesses à Aviemore - Cain (1978).

Table 2. Drag reduction experiments and air concentration boundary layer characteristics
Mesures des réductions du coefficient de frottement et de la couche limite de concentrations en air

References (1)	δ_{ab} mm (2)	Bubble size d_b mm (3)	C_b (4)	Velocity V_o m/s (5)	Comments (6)
Bogdevich et al. (1977)	0.7 to 3.4	0.002 to 0.1	0.14 to 0.7	4.3 to 10.9	Microbubble-modified boundary layer
Madavan et al. (1984)		0.005		4 to 17	Microbubble-modified boundary layer
Madavan et al. (1985)		0.0005 to 0.1		4 to 17	Microbubble-modified boundary layer
Marie et al. (1991)	2	4	0.02 to 0.07	0.5 to 1	Millimetric bubbles in a turbulent boundary layer on a flat plate
Cain (1978)	10 to 30	0.5 to 5	0.04 to 0.27	18 to 22	Self-aerated flows Prototype spillway
Chanson (1988)	15 to 23	0.3 to 4	0.15 to 0.27	9 to 17	Self-aerated flows Spillway model

Notes: δ_{ab} = air concentration boundary layer thickness
C_b = air concentration at the outer edge of the air concentration boundary layer
V_o = velocity outside the boundary layer

obtained for air concentrations C_b in the range 0.04 to 0.70. To a first approximation, it is reasonable to believe that equation (7) and Δ_{ab} do not depend upon the air concentration at the outer edge of the air concentration boundary layer. Further Fig. 4 shows that the boundary layer thickness Δ_{ab} increase with the Reynolds number $Re+$. It suggests also that Δ_{ab} might tend toward an asymptotic value of about $2 \cdot 10^4$ for large Reynolds numbers.

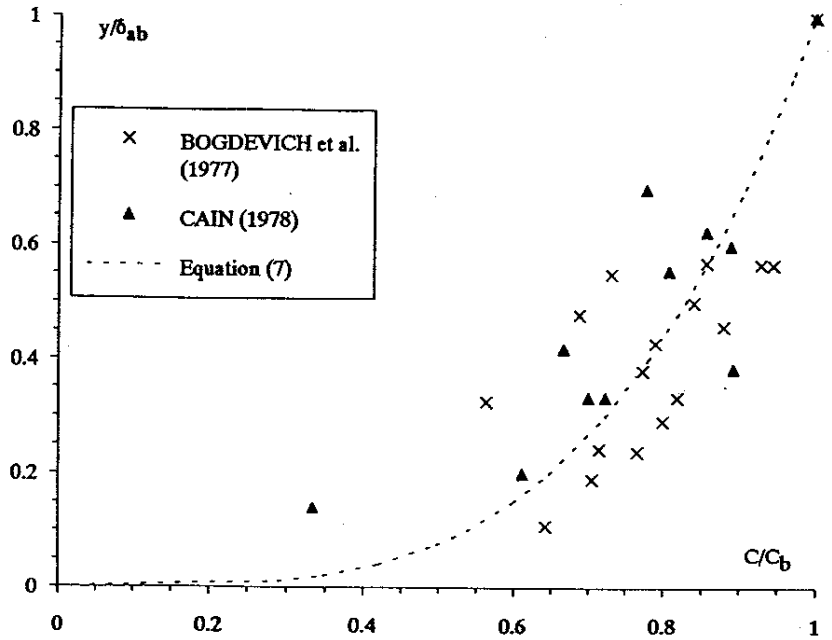

Fig. 3. Air concentration distribution in the air concentration boundary layer.
Concentrations en air dans le couche limite de concentration en air.

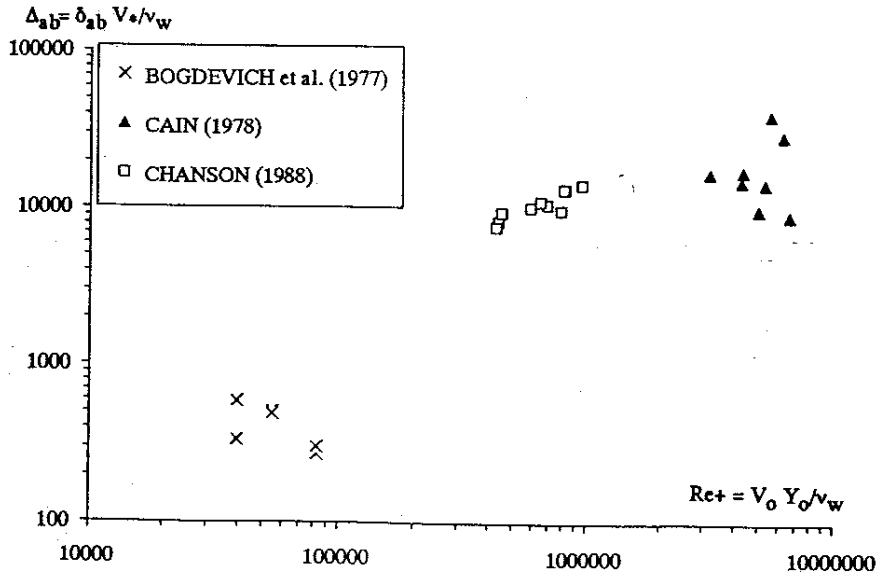

Fig. 4. Thickness of the air concentration boundary layer as a function of the Reynolds number.
Epaisseur de couche limite de concentration en air en fonction du nombre de Reynolds.

In self-aerated flows, velocity measurements obtained on a prototype spillway (Cain 1978) and on a spillway model (Chanson 1988) indicate that the velocity distribution of the air-water mixture is not affected by the presence of air bubbles. Cain and Wood (1981) showed that the velocity distribution can be approximated by:

$$\frac{V}{V_{90}} = \left(\frac{y}{Y_{90}}\right)^{1/n} \tag{8}$$

where V is the velocity at a distance from the invert and the exponent n, for the roughness of Aviemore dam, is : $n = 6.0$ (Chanson 1989). On Aviemore dam the non aerated friction factor computed from the Colebrook-White formula is in the range 0.022 to 0.023. Equation (8) was obtained with mean air concentrations in the range 0 to 50%.
For a given mean air concentration, the characteristic velocity V_{90} can be deduced by combining equations (6), (7) and (8) with the continuity equation for water. Results are given in Table 1, column 5.

3 Drag reduction in self-aerated flows

Presentation
The presence of air bubbles does not affect the velocity distribution but is expected to reduce the shear stress between the flow layers (Killen 1968, Wood 1983, Chanson 1992a). Wood (1983) showed that self-aeration induces a drag reduction which increases with the mean air concentration. The author (Chanson 1992a) re-analysed prototype and model data and the results showed that the drag reduction can be estimated as:

$$\frac{f_e}{f} = 0.307 + 0.1446 \log_{10}(Re) - 1.4 C_{mean} \tag{9}$$

where f is the non-aerated flow friction factor, f_e is the aerated friction factor, $Re = U_w D_H/\nu_w$ and D_H is the hydraulic diameter. Equation (9) was obtained for $C_{mean} > 0.25$ and Re in the range $2 \cdot 10^5$

to $4 \cdot 10^7$. Hartung and Scheuerlein (1970) studied open channel flows on rockfilled channels, with great natural roughness and steep slopes. The extremely rough bottom induced a highly turbulent flow with air entrainment. Their results indicated also a drag reduction due to the presence of air that may be expressed as:

$$\frac{f_e}{f} = \frac{1}{(1 - 3.2\sqrt{f}\log_{10}(1 - C_{mean}))^2} \tag{10}$$

Drag reduction on prototype spillways

The author re-analysed a new set of prototype data obtained in Australia, Austria, Indonesia, USA, USSR and Yugoslavia (Table 3) using the method introduced by Wood (1983) and extended by Chanson (1992a). For the model and prototype data, the drag reduction is estimated as:

$$\frac{f_e}{f} = 0.5\left(1 + \tanh\left(0.628\,\frac{0.514 - C_{mean}}{C_{mean}(1 - C_{mean})}\right)\right) \tag{11}$$

where $\tanh(x) = (\exp(x) - \exp(-x))/(\exp(x) + \exp(-x))$. The experimental data are presented in Fig. 5 and compared with equation (11). For these data the relative roughness k_s/D_H was in the range $3 \cdot 10^{-4}$ up to $4 \cdot 10^{-2}$ where k_s is the equivalent uniform sand roughness, and Re was in the range $5 \cdot 10^4$ to $3 \cdot 10^7$.

Fig. 5 shows that the aerated friction factor f_e departs from the non aerated value f for mean air concentrations larger than 20%. For $C_{mean} > 20\%$, the air concentration next to the chute invert (i.e. C_b, Table 1, column 4) becomes larger than zero, and the air bubbles start interacting with the shear layers next to the invert.

Table 3. Selft-aerated flow measurements on prototype and model spillways
Ecoulements à surface libre avec entraînement d'air: modèles et prototypes

Spillway (1)	Slope degrees (2)	q_w m²/s (3)	k_s/D_H (4)	Re (5)	Ref. (6)	Comments (7)
Prototype spillway						
Ak-Tepe, USSR	21.8	2.3 to 8.0	5E-3 to 1E-2	8.8E+6 to 2.8E+7	[A]	Rough concrete $W=5$ mm, $k_s=5$ mm
Aviemore, New Zealand	45.0	2.23 & 3.16	8E-4 to 1.9E-3	8.9E+6 to 1.3E+7	[CA]	Concrete $k_s=1$ mm
Bencok, Indonesia	31.05	2.9 to 6.0	3E-3 to 4.6E-3	9E+6 to 1.6E+7	[A, E, L]	$W=1$ m, $k_s=2$ mm
Big Hill, Australia	4.2	0.74 to 0.82	6.5E-3	2E+6	[M]	Smooth concrete
Boise, USA	4.6 to 12.2	0.01 to 0.8	2.7E-3 to 3.1E-2	5.3E+4 to 2.8E+6	[S]	Concrete, $W=0.9$ to 1.8 m, $k_s=1$ mm
Dago, Indonesia	13.8	0,74 to 1.39	2.5E-3 to 3.4E-3	2.5E+6 to 4.5E+6	[A, E, L]	$W=1$ m, $k_s=1$ mm
Erevan, USSR	21.8	0.38 to 1.55	1.9E-2 to 4E-2	1.5E+6 to 5.8E+6	[A]	Rough basalt and cement mortar $W=4$ m, $k_s=10$ mm

Table 3. continued

Spillway (1)	Slope degrees (2)	q_w m^2/s (3)	k_s/D_H (4)	Re (5)	Ref. (6)	Comments (7)
Gizel'don, USSR	28.1	0.49 to 1.28	5E-4 to 1.1E-3	1.9E+6 to 5E+6	[A]	Wooden flume $W=6$ m, $k_s=0.3$ mm
Hat Creek, USA	23.45 to 34.75	1.86 to 6.4	4.8E-3 to 1.2E-2	6E+6 to 2E+7	[H]	Rough concrete $W=1.75$ m, $k_s=5$ mm
Kittitas, USA	33.2	2.24 to 11.7	7E-3 to 2E-2	8E+6 to 3E+7	[H]	Eroded concrete $W=2.44$ m, $k_s=10$ mm
Mallnitz, Austria	22.2				[A, E, L]	Concrete $W=2$ m
Mostarsko, Blato, Yugoslavia		0.71 to 3.44	1.5E-2 to 3.5E-2	8.3E+4 to 3E+7	[J]	Stone lining $W=5.35$ mm, $k_s=20$ mm
Rapid Flume, USA	20.1	1.76	3E-4	6E+6	[H]	Wooden flume $W=1.4$ m, $k_s=0.1$ mm
Spring Gully, Australia	5.3		6E-3 to 7E-4	2E+6	[M]	Smooth concrete Semi circular ($R=0.61$ m)
Rutz, Austria	34	0.4 to 2	3E-4 to 1.3E-3	2E+ to 7E+6	[I]	Concrete Trapezoidal
Spillway	*models*					
Clyde model, New Zealand	52.3	0.21 to 0.48	3.8E-4 to 1.2E-3	8E+5 to 2E+6	[CH]	Perspex, D/S of aerator $W=0.25$ m, $k_s=0.1$ mm
IWP, USSR	16.7 & 29.7	0.064 to 0.13	1.3E-3 to 2.6E-3	2.3E+5 to 4.3E+5	[A]	Planed board with painting $W=0.25$ m, $k_s=0.1$ mm
Vienna Lab., Austria	8.7 to 31.2	0.04 to 0.178			[A, E, J, L]	Wooden flume $W=0.25$ m
St. Anthony Falls, USA	7.5 to 75	0.14 to 0.93	3E-3 to 1.6E-2	4.7+5 to 2E+6	[SA]	Artificial roughness $W=0.46$ m, $k_s=0.7$ mm
Rockfilled	*channels*					
Obernach, Germany	6 to 34		0.02 to 0.2		[HS]	$k_s=0.1$ to 0.35 m

Notes: [A] Aivazyan (1986); [CA] Cain (1978); [CH] Chanson (1988); [E] Ehrenberger (1926); [H] Hall (1943); [HS] Hartung and Scheuerlein (1970); [I] Innerebner (1924); [J] Jevdjevich and Levin (1953); [L] Levin (1955); [M] Michels and Lovely (1953); [S] Stewart (1913); [SA] Straub and Anderson (1958).

Discussion

An interesting aspect of the drag reduction in self-aerated flows is the interactions between the drag reduction, the velocity profile, and the air concentration distribution next to the chute invert. By analogy with dilute polymer solutions (Virk 1975, Lumley 1977) and bubble-modified boundary layers (Bogdevich et al. 1977, Marie et al. 1991), the air concentration boundary layer might play a role similar to the elastic sub-layer and viscous sublayer in the drag reduction process. The presence of air bubbles next to a solid boundary (e.g. invert, flat plate) increases the effective dynamic viscosity, resulting in a thickening of the viscous sublayer (Lumley 1977, Marie 1987).

Marie (1987) developed an analytical model to predict the drag reduction due to the presence of air bubbles next to the wall. This model is based on the thickening of the sublayer due to the

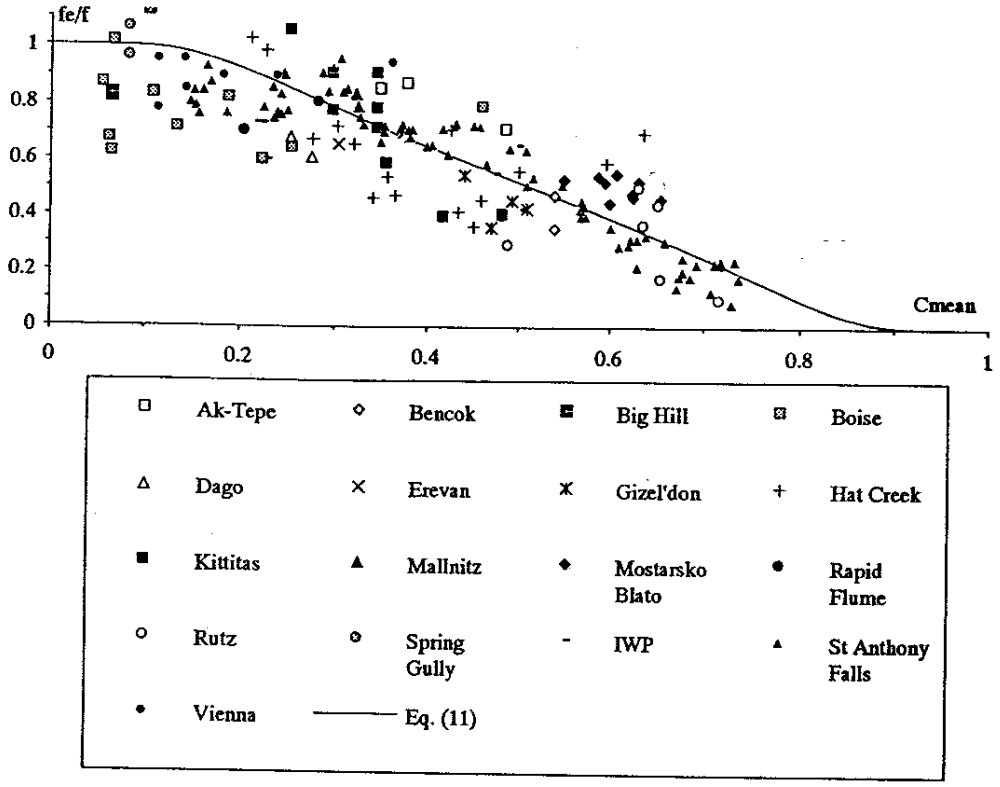

Fig. 5. Drag reduction observed on prototype spillways and spillway models.
Réduction du coefficient de frottement sur des modèles et prototypes.

increase of kinematic viscosity of the air-water flow next to the boundary. The density of air is 1000 time less than the density of water. In the flow layers close to the boundary, the effective density of the air-water mixture can be approximated as:

$$\varrho_{aw} = \varrho_w(1 - C_b) \tag{12}$$

where ϱ_{aw} is the air-water density and C_b is the air concentration at the outer edge of the air concentration boundary layer. Einstein (1906, 1911) proved that the effective viscosity can be estimated as:

$$\mu_{aw} = \mu_w(1 + 2.5 * C_b) \tag{13}$$

where μ_{aw} is the effective viscosity of the air-water mixture and μ_w is the water viscosity. Using equations (12) and (13), Marie's (1987) calculations yield to:

$$\frac{f_e}{f} = \left(1 + \sqrt{\frac{f}{8}}\left(10.5\left(\frac{1 + 2.5C_b}{1 - C_b} - 1\right) - 2.44\,\mathrm{Ln}\left(\frac{1 + 2.5C_b}{1 - C_b}\right)\right)\right)^{-9/5} \tag{14}$$

Equation (14) is plotted on Fig. 6 as a function of the mean air concentration for several values of the non-aerated friction factor, using the air concentration at the outer edge of the air concentration boundary layer C_b (Table 1, column 4). In the air concentration boundary layer, experimental data (Cain 1978, Chanson 1988, 1992b) and calculations (Chanson 1992c) indicate that the bubble sizes are small (i.e. $d_b < 1$ mm) next to the spillway invert. These values are of the same order of magnitude as the experiments of Bogdovich et al. (1977) and Madavan et al. (1984, 1985) used to verify Marie's (1987) model (Table 2). Therefore it is relevant to compare equations (11) and (14)

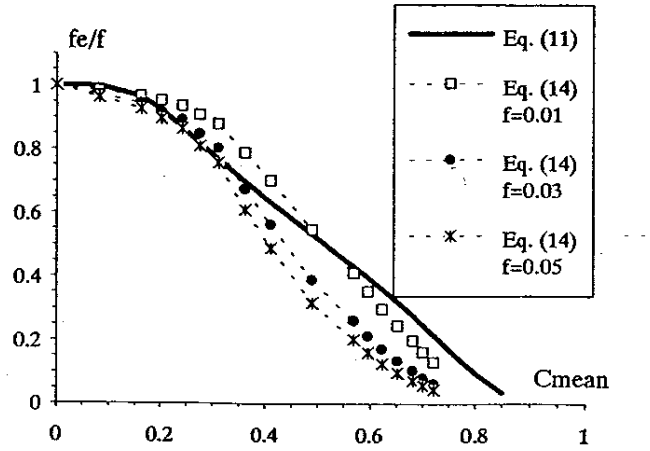

Fig. 6. Drag reduction: comparison between equations (11) and (14).
Comparaisons entre les équations (11) et (14).

as shown on Fig. 6. The agreement between these equations is good and confirms the analogy between the mechanisms of drag reduction.

The author (Chanson 1992b) suggested that the small air bubbles observed in the air concentration boundary layer act as rigid spheres (Comolet 1979) and offer a large resistance to break up under the action of turbulent shear stress. It is believed that such rigid air bubbles behave as macro-molecules of polymer and block the turbulence bursting processes in the air concentration boundary layer as macro-molecules do in the viscous sub-layer (Virk 1975). Further dilute polymer solutions can exhibit macromolecular elongation characteristics that induce an increase of viscosity in the outer region of the sublayer called the elastic sublayer (Virk 1975, Tam et al. 1992). In air-water flows the presence of air bubbles at the outer edge of the air concentration boundary layer and their absence at the solid boundary is similar to the presence of elongated macromolecules in the elastic sublayer. Air bubbles and elongated macromolecules increase the viscosity and "this increase in viscosity, in the turbulent part and not in the viscous sublayer, suppresses the eddies which carries the Reynolds stress in the buffer layer, resulting in a thickening of the sublayer, and a reduction in drag" (Lumley 1977).

It must be noted that Lumley's conclusion emphasises the role of the air concentration boundary layer in the drag reduction process taking place in self-aerated flows.

Analogy with suspended sediment flows

In laboratory and river flows, suspended sediment is observed to increase the flow velocity and to decrease the friction factor (Buckley 1923, Vanoni 1946, Vanoni and Nomicos 1960, Graf 1971). Despite controversies, the velocity distribution in the inner flow region follows the classical logarithmic profile (Coleman 1981, Lynn 1988) and exhibits a viscous sublayer. By analogy with air-water flows and dilute polymer solutions, it is believed that the presence of suspended particles might induce a thickening of the sublayer and a reduction of bottom shear stress.

The presence of sediment particles, in the flow layers next to the bottom, increases the density and the viscosity of the flow. At the outer edge of the viscous sublayer, the density of sediment laden flow ϱ_{sw} is:

$$\varrho_{sw} = \varrho_w \left(1 + C_{sb} \left(\frac{\varrho_s}{\varrho_w} - 1\right)\right) \tag{15}$$

where ϱ_s is the sediment density and C_{sb} is the volumetric concentration of sediment next to the bed. If the suspension is stable, the dynamic viscosity of the sediment-water mixture μ_{sw} can be estimated as (Graf 1971):

$$\mu_{sw} = \mu_w(1 + 2.5C_{sb} + (2.5C_{sb})^2 + ...) \tag{16}$$

for volume concentration up to 35%. Combining equations (15) and (16), the kinematic viscosity of the sediment-water mixture increases with the concentration for $\varrho_s < 3.5$. Marie's (1987) model would predict a drag reduction as:

$$\frac{f_s}{f} = \left(1 + \sqrt{\frac{f}{8}}\left(10.5\left(\frac{1 + 2.5C_{sb} + 6.25C_{sb}^2}{1 + C_{sb}\left(\frac{\varrho_s}{\varrho_w} - 1\right)} - 1\right) - 2.44\,\mathrm{Ln}\left(\frac{1 + 2.5C_{sb} + 6.25C_{sb}^2}{1 + C_{sb}\left(\frac{\varrho_s}{\varrho_w} - 1\right)}\right)\right)\right)^{-9/5} \tag{17}$$

where f_s is the friction factor of suspended sediment flows. On Fig. 7, model and prototype data are presented as a function of the mean volumetric sediment concentration C_s assuming a sediment density of 2500 kg/m^3. Details of the flow conditions are given in Table 4. Vanoni's (1946, 1960) experiments, presented on Fig. 7, were performed with suspended sediments without depositing material. For these data, equation (17) was computed using the sediment concentration measured at a distance [0.05 d] above the bed and are plotted on Fig. 7 as a function of the mean sediment concentration C_s. The results are in reasonable agreement with the model data. It must be noticed that the data of Buckley (1923) must be considered with great care as the changes in friction factor due to variation in bed configuration might be important.

By analogy with air-water shear flows and dilute polymer solutions, an increase of the viscosity in the flow layers next to the boundary might explain the observed drag reduction in suspended particle flows. But it must be emphasised that the sediment concentration increases toward a maximum at the channel bottom and no concentration boundary layer is observed.

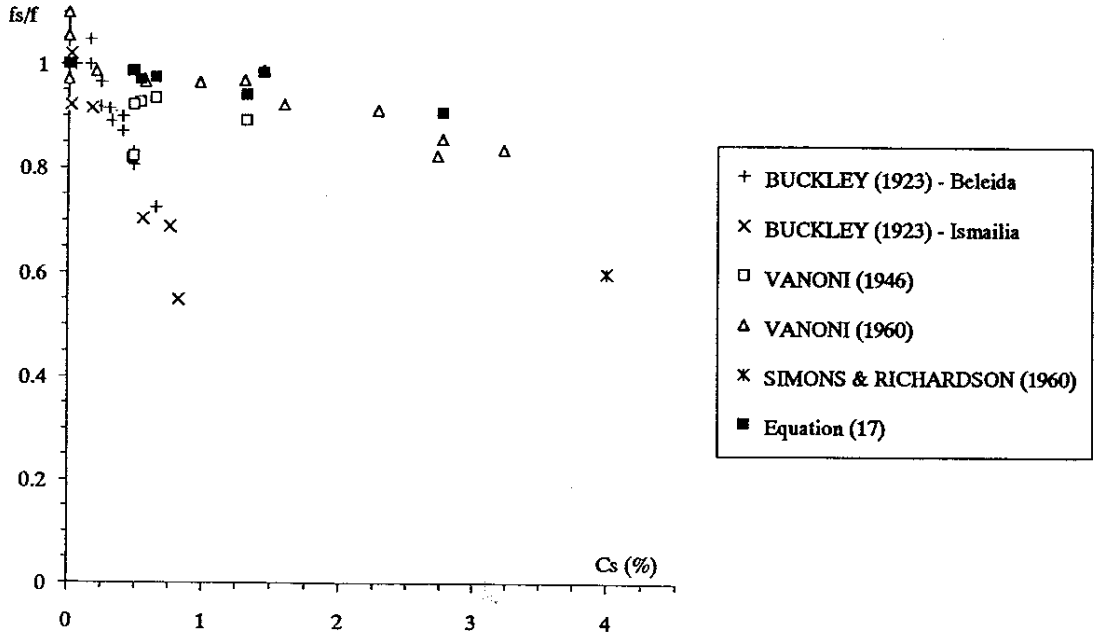

Fig. 7. Drag reduction observed in sediment laden flows (Buckley 1923, Vanoni 1946–1960, Simons and Richardson 1960).

Réduction du coefficient de frottement pour des écoulements avec suspension de matériaux (Buckley 1923, Vanoni 1946–1960, Simons et Richardson 1960).

Table 4. Suspended sediment flow measurements on models and prototypes
Ecoulements avec matériaux en suspension: modèles et prototypes

Reference (1)	Discharge m^3/s (2)	C_s (3)	U_w m/s (4)	Comments (5)
Buckley (1923)	900 to 6700 47 to 68	120 to 1,620 g/m^3 14 to 2,050 g/m^3	0.5 to 1.4 0.52 to 0.68	Prototype data. Nile river at Beleida discharge station. Prototype data. Canal derivation from the Nile river.
Vanoni (1946)	0.03 to 0.15	0 to 3,190 g/m^3	0.55 to 1.2	Model data. $W=0.84$ m
Vanoni and Nomicos (1960)	0.014	0 to 8,100 g/m^3	0.69 to 0.70	Model data. $W=0.27$ m
Simons and Richardson (1960)		40,000 ppm		Fine sediments (clays)

Notes: C_s average sediment concentration
U_w average flow velocity
W channel width

4 Conclusion

The characteristics of self-aerated flows are developed for chute spillways. In particular self-aeration induces a substantial reduction of the friction factor on both models and prototypes, Although the velocity distribution is not affected by the presence of air bubbles, the shape of the air concentration distribution shows the presence of an air concentration boundary layer next to the spillway bottom (equation (7)). The air concentration boundary layer plays a major role in the drag reduction process. By analogy with dilute polymer solutions and microbubble modified boundary layers, it is suggested that the presence of air next to the invert increases the effective viscosity of the mixture and the sublayer thickness, and induces drag reduction (equation (11)) as observed on prototypes. The analysis of model and prototype data indicate that the drag reduction can be as large as 80% (Fig. 5).
A similar mechanism might explain also the mechanism of drag reduction observed in sediment laden flows.

List of symbols

B' integration constant of the equilibrium air concentration distribution
C air concentration defined as the volume of air per unit volume
C_b air concentration next to the spillway bottom at the outer edge of the air concentration boundary layer
C_s mean volumetric sediment concentration
C_{sb} volumetric sediment concentration at the outer edge of the viscous sublayer
C_{mean} depth averaged air concentration defined as: $(1 - Y_{90})C_{mean} = d$
D_H hydraulic diameter (m) defined as:

$$D_H = 4\frac{dW}{W + 2d}$$

d characteristic depth (m) defined as: $d = \int_{C=0\%}^{C=90\%} (1 - C)\, dy$

d_b air bubble diameter (m)

Fr Froude number defined as: $Fr = \frac{q_w}{\sqrt{g d^3}}$

f friction factor of non-aerated flow

f_e friction factor for aerated flow

f_s friction factor of suspended laden flow

G' integration constant of the equilibrium air concentration distribution

g gravity constant (m/s^2)

k_s equivalent uniform sand roughness (m)

n exponent of the velocity power law

Q discharge (m^3/s)

q discharge per unit width (m^2/s)

Re Reynolds number defined as: $Re = \varrho_w \frac{U_w D_H}{\mu_w}$

$Re+$ Reynolds number of boundary layer flows: $Re+ = \varrho_w \frac{V_o Y_o}{\mu_w}$

Note: for self-aerated flows $Re+ = \varrho_w \frac{V_{90} Y_{90}}{\mu_w}$

U_w flow velocity (m/s): $U_w = q_w/d$

u_r bubble rise velocity (m/s)

V velocity (m/s)

V_o free stream velocity (m/s) outside of the boundary layer

V_{90} characteristic velocity at Y_{90} (m/s)

V_* shear velocity (m/s)

v' root mean square of lateral component of turbulent velocity (m/s)

W channel width (m)

Y_o boundary layer thickness (m)

Y_{90} characteristic depth (m) where the air concentration is 90%

y distance from the bottom measured perpendicular to the spillway surface (m)

y' dimensionless depth: $y' = y/Y_{90}$

α spillway slope

Δ_{ab} dimensionless air concentration boundary layer thickness: $\Delta_{ab} = \varrho_w \frac{\delta_{ab} V_*}{\mu_w}$

δ_{ab} air concentration boundary layer thickness (m)

μ dynamic viscosity (N.s/m^2)

ν kinematic viscosity (m^2/s)

ϱ density (kg/m^3)

σ surface tension between air and water (N/m)

Subscript

air air flow

aw air-water flow

s sediment

sw sediment laden flow

w water flow

References / Bibliographie

AIVAZYAN, O. M. (1986), Stabilized Aeration on Chutes, Gidrotekhnicheskoe Stroitel'stvo, No. 12, pp. 33-40 (Hydrotechnical Construction, 1987, Plenum Publ., pp. 713-722).

BOGDEVICH, V. G., EVSEEV, A. R., MLYUGA, A. G. and MIGIRENKO, G. S. (1977), Gas-Saturation Effect on Near-Wall Turbulence Characteristics, Proc. of the 2nd Intl. Conf. on Drag Reduction, BHRA Fluid Eng., Cambridge, UK, Paper D2, pp. 25-37.

BUCKLEY, A. B. (1923), The Influence of Silt on the Velocity of Water Flowing in Open Channels, Minutes of the Proc. Instn Civ. Engrs., 1922-1923, Vol. 216, Part II, pp. 183-211, Discussion, pp. 212-298.

CAIN, P. (1978), Measurements within Self-Aerated Flow on a Large Spillway, Ph.D. Thesis, Ref. 78-18, 1978, Univ. of Canterbury, Christchurch, New Zealand.

CAIN, P. and WOOD, I. R. (1981), Measurements of Self-aerated Flow on a Spillway, J. Hyd. Div., ASCE, 107, HY11, pp. 1425-1444.

CHANSON, H. (1988), A Study of Air Entrainment and Aeration Devices on a Spillway Model, Research Rep. 88-8, Oct., Univ. of Canterbury, New Zealand.

CHANSON, H. (1989), Flow downstream of an Aerator, Aerator Spacing, Jl. of Hyd. Research, IAHR, Vol. 27, No. 4, pp. 519-536.

CHANSON, H. (1992a), Entraînement d'Air dans les Ecoulements à Surface Libre: Application aux Evacuateurs de Crues de Barrage (Air Entrainment in Open Channel Flow: Application to Spillways), J. La Houille Blanche, No. 4, 1992, pp. 277-286 (in French).

CHANSON, H. (1992b), Discussion of 'A General Correlation for Turbulent Velocity Profiles of Dilute Polymer Solutions', by K. C. Tam, C. Tiu and R. J. Keller, J. of Hyd. Res., IAHR, Vol. 30, No. 1, 1992, pp. 117-142, J. of Hyd. Res., IAHR, Vol. 30, No. 6.

CHANSON, H. (1992c), Air Entrainment in Chutes and Spillways, Research Report No. CE 133, Dept. of Civil Engineering, University of Queensland, Australia, Feb., 85 pages.

COLEMAN, N. L. (1981), Velocity Profiles with Suspended Sediment, J. of Hyd. Res., IAHR, Vol. 19, No. 3, pp. 211-229.

COMOLET, R. (1979), Sur le Mouvement d'une bulle de gaz dans un liquide, (Gas bubble motion in a liquid medium), J. La Houille Blanche, 1979, No. 1, pp. 31-42 (in French).

EHRENBERGER, R. (1926), Wasserbewegung in steilen Rinnen (Susstennen) mit besonderer Berucksichtigung der Selbstbelüftung, (Flow of Water in Steep Chutes with Special Reference to Self-aeration), Zeitschrift des Österreichischer Ingenieur und Architektverein, No. 15/16 and 17/18 (in German) (translated by Wilsey, E. F., U.S. Bureau of Reclamation).

EINSTEIN, A. (1906), Eine Neue Bestimmung der Moleküldimensionen, Ann. Phys., 19, p. 289.

EINSTEIN, A. (1911), Eine Neue Bestimmung der Moleküldimensionen, Ann. Phys., 34, p. 591.

ERVINE, D. A. and FALVEY, H. T. (1987). Behaviour of Turbulent Water Jets in the Atmosphere and in Plunge Pools, Proc. Instn Civ. Engrs., Part 2, Mar. 1987, 83, pp. 295-314.

FALVEY, H. T. (1980), Air-Water Flow in Hydraulic Structures, USBR Engrg. Monograph, No. 41, Denver, Colorado, USA.

GRAF, W. H. (1971), Hydraulics of Sediment Transport, McGraw-Hill, New York, USA.

HALL, L. S. (1943), Open Channel Flow at High Velocities, Trans. ASCE, Vol. 108, pp. 1394-1434.

HARTUNG, F. and SCHEUERLEIN, H. (1970), Design of Overflow Rockfill Dams, 10th ICOLD Congress, Montréal, Canada, Q.36, R.35, pp. 587-598.

INNEREBNEK, K. (1924), Overflow Channels from Surge Tanks, World Power Conference, 1st, Vol. 2, pp. 481-486.

JEVDJEVICH, V. and LEVIN, L. (1953), Entrainment of Air in flowing Water and Technical Problems connected with it, Proc. of 5th I.A.H.R. Congress, IAHR-ASCE, Minneapolis, USA, pp. 439-454.

KILLEN, J. M. (1968), The Surface Characteristics of Self-Aerated Flow in Steep Channels, Ph.D. thesis, University of Minnesota, Minneapolis, USA.

LEVIN, L. (1955), Quelques Réflexions sur la Mécanique de l'écoulement des Mélanges d'Eau et d'Air, (Notes on the Flow Mechanics of Water-Air Mixtures), J. La Houille Blanche, No. 4, Aug.-Sept., 1955, pp. 55-557 (in French).

LUMLEY, J. L. (1977), Drag Reduction in Two Phase and Polymer Flows, Physics Fluids, Vol. 20, No. 10, Pt II, pp. S64-S71.

LYN, D. A. (1988), A Similarity Approach to Turbulent Sediment-Laden Flows in Open Channels, J. Fluid Mech., Vol. 193, pp. 1-26.

MADAVAN, N. K., DEUTSCH, S. and MERKLE, C. L. (1984), Reduction of Turbulent Skin Friction by Microbubbles, Physics Fluids, Vol. 27, No. 2, pp. 356-363.

MADAVAN, N. K., DEUTSCH, S. and MERKLE, C. L. (1985), Measurements of Local Skin Friction in a Microbubble-Modified Turbulent Boundary Layer, J. Fluid Mech., Vol. 156, pp. 237–256.

MARIE, J. L. (1987), A Simple Analytical Formulation for Microbubble Drag Reduction, PCH, Vol. 8, No. 2, pp. 213–220.

MARIE, J. L., MOURSALI, E. and LANCE, M. (1991), A First Investigation of a Bubbly Boundary Layer on a Flat Plate: Phase Distribution and Wall Shear Stress Measurements, Proc. of the 1st ASME-JSME Fluids Eng. Conf., Turbulence Modification in Multiphase Flows 1991, June, Portland, USA, FED-Vol. 110, ASME, pp. 75–80.

MAY, R. W. P. (1987), Cavitation in Hydraulic Structures: Occurrence and Prevention, Hydraulics Research Report, No. SR 79, Wallingford, UK.

MICHELS, V. and LOVELY, M. (1953), Some Prototype Observations of Air Entrained Flow, Proc. of 5th I.A.H.R. Congress, AIHR-ASCE, Minneapolis, USA, pp. 403–414.

SENE, K. J. (1984), Aspects of Bubbly Two-Phase Flow, Ph.D. thesis, Trinity College, Cambridge, UK, Dec.

SIMONS, D. B. and RICHARDSON, A. M. (1960), Resistance Properties of Sediment-Laden Streams, Discussion, Trans. ASCE, Vol. 125, Part I, pp. 1170–1172.

STEWART, W. G. (1913), The Determination of the N in Kutter's Formula for Various Canals, Flumes and Chutes on the Boise Project and Vicinity, Report on 2nd Annual Conf. on Operating Men, USBR, Boise, Idaho, USA, Jan., pp. 8–23.

STRAUB, L. G. and ANDERSON, A. G. (1958), Experiments on Self-Aerated Flow in Open Channels, J. of Hyd. Div., Proc. ASCE, Vol. 84, No. HY7, paper 1890.

TAM, K. C., TIU, C. and KELLER, R. J. (1992), A General Correlation for Turbulent Velocity Profiles of Dilute Polymer Solutions, J. of Hyd. Res., IAHR, Vol. 30, No. 1, pp. 117–142.

VANONI, V. A. (1946), Transportation of suspended sediment in water, Trans. ASCE, Vol. 111, pp. 67–133.

VANONI, V. A. and NOMICOS, G. N. (1960), Resistance Properties of Sediment-Laden Streams, Trans. ASCE, Vol. 125, Part I, pp. 1140–1167.

VIRK, P. S. (1975), Drag Reduction Fundamentals, AIChE J., Vol. 21, No. 4, pp. 625–656.

WOOD, I. R. (1983), Uniform Region of Self-Aerated Flow, J. Hyd. Eng., ASCE, Vol. 109, No. 3, pp. 447–461.

WOOD, I. R. (1984), Air Entrainment in High Speed Flows, Proc. of the Intl. Symp. on Scale Effects in Modelling Hydraulic Structures, IAHR, Esslingen, Germany, H. Kobus editor, paper 4.1.